Range Errors due to Occlusion in Non-Coaxial LADARs

Bingbing Liu[†], Martin Adams[†], Javier Ibañez-Guzmán[♮] and Wijerupage Sardha Wijesoma[†]
[†]*School of Electrical & Electronics Engineering, Nanyang Technological University, Singapore.*
[♮]*SIMTech, 71 Nanyang Drive, Singapore.*
Email: [†]{pg01604923, eadams, eswwijesoma}@ntu.edu.sg, [♮]javierg@SIMTech.a-star.edu.sg

***Abstract*— A prerequisite for mobile robot navigation is a reliable sensing mechanism. Laser detection and ranging sensors or LADARs are widely used in mobile robotics. When processing LADAR data for the purposes of feature extraction and/or data association, most previous work models such devices as processing range data which follows a Normal distribution. In this paper, it will be demonstrated that commonly used LADARs suffer from incorrect range readings at range discontinuities, which can have a much more detrimental effect on feature extraction or data association algorithms than random noise.**

LADARs with separated transmitter and receiver configuration can introduce a significant occlusion effect, as the reflected laser energy from the target can be partially occluded from the receiver. This paper will demonstrate that false range values can result from LADARs and that the occurrence of these values can be reliably predicted by monitoring the received signal strength. A useful design criterion for the optical separation of the transmitter and receiver is also derived for non-coaxial LADARs and the exact environmental conditions which can cause range errors is quantified so that such errors can be reliably predicted.

I. Introduction

In mobile robotics, range sensing is often a crucial component of navigational and localization tasks [6], [4]. Laser detection and ranging sensors, or LADARs, with range and bearing information, have become an integral component of many autonomous systems due to their accuracy and relatively low cost.

The work in this paper is inspired by the processing of LADAR range data for the detection of features for mobile robot navigation [1], [8], [12]. Such algorithms are often based on probabilistic methods which attempt to extract information from the range data in an optimal manner, on the assumption that the range data is corrupted with Gaussian noise. For example Guivant *et al* have made an observation model for their Kalman filter based outdoors navigation system, by assuming Gaussian noise [6]. Adams was able to detect range/reflectance discontinuities, by optimally weighting new range data with simple recursive line and constant curvature models - also based on range data Gaussian noise assumptions [1].

In the experience of the authors, such feature extraction algorithms often fail due to other systematic, unmodelled errors from LADARs. For example, Kalman Filter based and scale space detection algorithms [12], [11] can fail catastrophically when range errors due to *cross talk* [9], *disparity* [10] or *multi-path effects* [1] occur. Removing such "outliers" from range data can be achieved with limited success with standard techniques such as median filters [5], based on certain assumptions about the erroneous range data. This paper will demonstrate that significant range errors can occur due to occlusion caused by a combination of transmitter and receiver (transceiver) separation and the scanning reflection principle[1].

Firstly, the 3D scanning LADAR systems used in this work will be presented in section II. Then, in section III an overview of the problem will be demonstrated with range/intensity data recorded from a scanning LADAR. It will be shown that significant range errors occur at, or near, range discontinuities, which have a detrimental effect on feature detection algorithms which attempt to isolate such range/intensity changes and then use such 'end' range points for future data association [7]. The physical cause of this effect will be studied in detail in section IV and a theoretical model will be derived which allows such errors to be predicted and detected from range scans. In particular it will be shown that the amplitude of the received signal will follow well defined profiles as the scanning mirror rotates, which depends on the orientation of the scanning mirror relative to the LADAR's transmitting and reception apertures. The theoretical analysis applies to all detection methods, since the range errors occur due to a significant drop in received signal amplitude. Then in section V, the theoretical model derived in section IV are analyzed to determine the parameters which cause the range errors. Experimental results are shown in section VI which demonstrate that such spurious range points can be reliably detected, provided the signal amplitude and orientation of the scanning optics and some environmental factors are monitored with each range data value.

II. 3D Scanning LADAR Systems

Two LADAR systems used in this work. The main LADAR system is based on a 1D Riegl LD90-3300EHS-FLP model, as shown in figure 1(a). This sensor is a time-of-flight (TOF) one with a reported maximum range measurement capability of 400m. For robot navigation, a desirable feature of any ranging system is that it provides full 360^o coverage around the robot in bearing, so that all objects within the field of view of the sensor can be

[1]to the authors' knowledge, an effect previously not examined for LADARs in the literature.

(a) (b) (c)

Fig. 1. (a) 1D Riegl LADAR LD90-3300EHS-FLP, (b) in-house developed 3D scanning mechanism and (c) 3D Riegl LADAR LMS-Z210i. The 3D mechanism in (b) and the 3D LADAR in (c) allow continuous rotation of the scanning mirror about the vertical axis and simultaneous control of the mirror's elevation about a horizontal axis.

"seen" from any vehicle orientation. Figure 1(b) shows a 3D scanning system developed at Nanyang Technological University (NTU) for this purpose. The 1D LADAR in figure 1(a) is mounted inside this system to perform as a 3D LADAR scanner.

The 3D LADAR shown in figure 1(c) is a LMS-Z210i model from Riegl. Its rather slow rotating rate[2] prevents it to be used in mobile robots. However, in this work, this kind of 3D LADAR is still used for comparison.

III. Range Errors in LADARs

Reported range errors in LADARs are due to cross talk and random noise [9], [1], [3]. A third type of error which has received attention in triangulation systems, but has not been analyzed in LADAR systems, is occlusion.

Figure 2 shows an intensity image[3] recorded from the 3D Riegl LADAR (figure 1(c)) in a laboratory environment.

Fig. 2. Received signal amplitude image recorded in a laboratory environment. Each pixel value is proportional to the received signal amplitude. The small circle (labelled with "A") shows a zero-signal amplitude point.

In figure 2 the small blue circle is shown to denote zero, or extremely low received signal amplitude values. These can be seen more clearly in figure 3 where the range and amplitude of the received signal is plotted versus the scanning mirror's bearing angle. This is taken from the middle row of pixels (elevation angle = 40^o) of figure 2. When the amplitude reaches zero (or extremely low values)

[2]At the fastest rotating rate, it takes around 20 seconds for the LADAR to fulfil a single 2D scan.

[3]received signal amplitude. In the paper, the two words "intensity" and "amplitude" or "signal amplitude" will be used interchangeably. The intensity is a ratio, which is a dimensionless quantity that ranges from 0 (least reflective) to 255 (most reflective) which is based on the strength of the return signal.

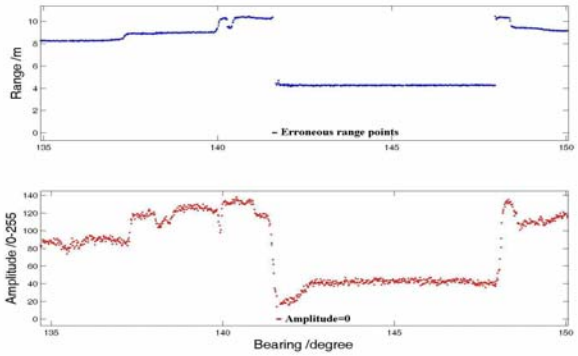

Fig. 3. Range (above) and received signal amplitude (below) versus bearing corresponding to the middle row (elevation angle being 40^o) of figure 2. Plots are shown here with bearing ranging only from 135^o to 150^o to clearly show the 0 amplitude and erroneous range reading points.

it can be seen that false ranges (range estimate = 0m) occur. These could, of course easily be detected as being false if their values were always zero. In reality, LADARs such as those from Riegl, Acuity Research and Sick[4] respond in different ways to such range discontinuities. It will be proved in section IV that *all* scanning LADARs with separated transmitter and receiver configurations will suffer a minimum in received signal amplitude due to the disparity between the transceiver aperture *irrespective of the technique used to estimate range*. And this paper will present a method to reliably predict such range failures.

The effect of disparity or the "missing parts" problem in triangulation systems has been well documented [10], however its subtle effect during the scanning of a LADAR and the resulting received amplitude profile does not appear to have been reported. Very few articles address the causes and effects of range errors in LADARs which can have a large impact on feature detection and data association algorithms. Notable exceptions are papers by Hebert and Krotkov [9], Reina and Gonzalez [2] and more recent articles by Cang and Borenstein [3]. These articles address the issues of range errors caused by *random receiver/reflection noise*, *cross talk* and *multiple path reflections*.

IV. Occlusion due to Transceiver Separation

In order to predict what sensor and environmental parameters will cause range errors due to occlusion, the physics of scanning will be studied in this section.

To study the occlusion effect, an experimental setup was made as shown in figure 4. To position the 1D LADAR in figure 1(a) precisely and to slide it in a controlled manner in a direction parallel to the target surfaces, it was mounted on the stacker of a milling machine and was translated to scan the edge of two targets as shown in 4(a). The range and amplitude information were recorded and for one particular experiment, are shown in figure 5. A minimum in the amplitude profile occurs because of the separated transceiver configuration of the sensor. There

[4]LADARs commonly used in mobile robotics research.

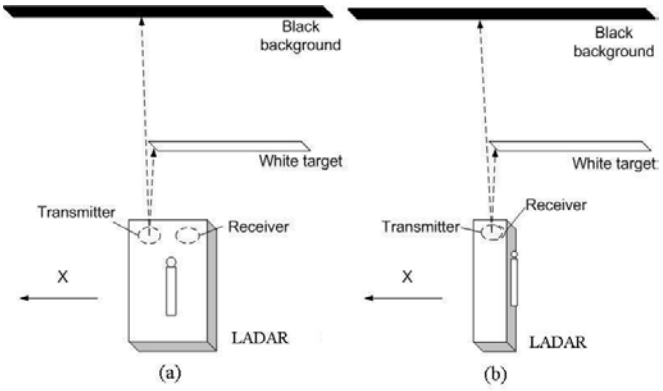

Fig. 4. (a) The LADAR is displaced past on an edge formed by a target and a background. (b) The sensor is rotated 90° right so that the transmitter and the receiver are displaced "coaxial" to the edge .

is a loss in received energy due to the non-coaxiality of the sensor. When the amplitude drops below the minimum working threshold of the LADAR, the range reading cannot be trusted (it often reads zero for these two LADARs in figure 1 but in general it may read any arbitrary value and hence cannot be compensated by a simple low-pass filter). This is the occlusion effect. Most LADAR sensors fall into two categories: coaxial (e.g. most Sick LADARs) or separated (e.g. most Riegl LADARs) transceiver configurations. These configurations determine whether or not occlusion occurs.

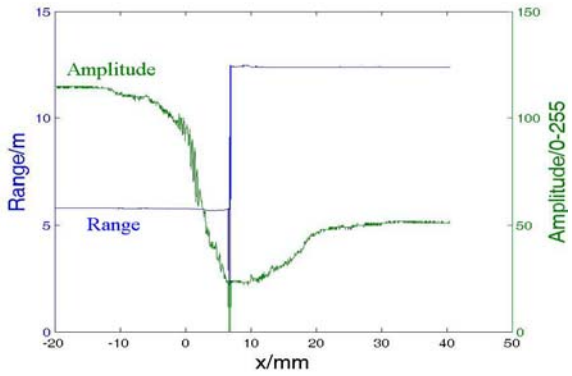

Fig. 5. Range and amplitude when the 1D LADAR is translated on a stacker to scan an edge.

The following analysis will mathematically derive the profile of the received signal power from these two LADARs, as their scanning mirrors rotate so that the transmitted laser is scanned past a range discontinuity. It will then be shown how this profile can be used to predict when range errors will occur and how to detect them. In the analysis, the following assumptions are made:

1) The power in the transmitted and reflected light beams is uniformly distributed over the circular, cross-sectional area of the LADAR.[5]

[5]Note that the following analysis could be easily extended to other non-uniform optical power distributions.

2) Assumptions 1 allows us, without loss of generality, to model the scanning procedure with targets 1 and 2 parallel to the motion of the LADAR, irrespective of their true orientation.
3) Due to assumption 3, the rotational, scanning motion of the LADAR's mirror can be modelled as a linear displacement of the LADAR's optical footprint past the edge.

Initially, before the transmitted optical footprint intersects the edge, it will fully illuminate target 1 at range d_1, as shown in figure 6(a). In this case, the received

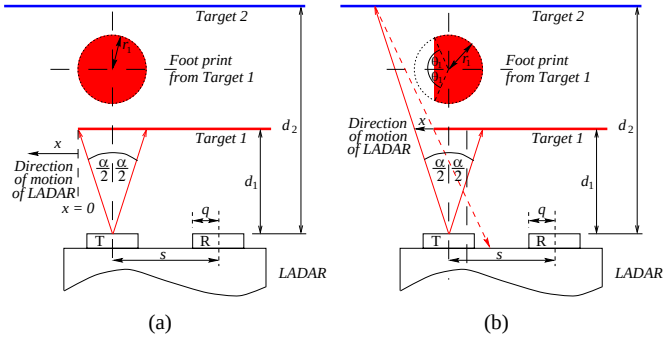

Fig. 6. (a) Only target 1 is illuminated. (b) Target 2 is completely occluded due to the transmitter – receiver separation s. The footprint's area on target 1 is reduced.

signal strength is P_1 watts, which can be measured if the amplitude of the received signal is available (as in the case of the Riegl and some Sick devices). As the mirror scans, the projected optical footprint will eventually completely traverse the edge, so that it fully illuminates target 2 at range d_2. In this case we assume that the received signal strength is P_2 watts (figure 7(d)).

In figures 6(a) and 7(d) we define the *end condition* received power *densities* as:

$$\mathcal{P}_{(x\leq 0)} = P_1/\pi r_1^2 \quad \mathcal{P}_{(x\geq X_2)} = P_2/\pi r_2^2 \qquad (1)$$

where x is the motion of the LADAR measured from the edge of target 1 and r_1 and r_2 are the radii of the normal components of the optical footprints on targets 1 and 2 respectively. The point $x = 0$ is defined when the transmitted light beam just reaches the edge of target 1, as shown in figure 6(a). The scanning of the LADAR's mirror is then considered to be equivalent to displacing the LADAR in the direction shown in figures 6(a) to (b) and figures 7 (a) to (d).

1) **LADAR displacement $x \leq 0$ (figure 6a).** The received signal power is given by:

$$P_{(x\leq 0)} = \mathcal{P}_{(x\leq 0)}\pi r_1^2 = P_1 = \text{constant} \qquad (2)$$

Define X_1 as being the value of x at which target 2 just becomes visible to the receiver aperture. This scenario is depicted in figure 7(a):

$$X_1 = (s-q)(d_2-d_1)/d_2 \qquad (3)$$

where s is the transmitter – receiver aperture separation and q is the effective radius of the receiver lens.

2) **LADAR displacement** $0 \leq x < X_1$ **(figure 6(b))**.The received power in this interval is:

$$P_{(0\leq x<X_1)} = P_1\left(1-\frac{\theta_1}{\pi}+\frac{\sin 2\theta_1}{2\pi}\right)$$
$$\theta_1 = \cos^{-1}\left(1-\frac{2x}{d_1\alpha}\right) \quad (4)$$

Equations 4 define the received power amplitude profile, which is expected when traversing the edge for $0 \leq x < X_1$.

3) **LADAR displacement** $X_1 \leq x < 2r_1$ **(figure 7(b)).** The power received in the displacement interval $X_1 \leq x < 2r_1$ results from the *two* footprint sections shown in figure 7(b) and is

$$P_{(X_1\leq x<2r_1)} = P_1\left[1-\frac{\theta_1}{\pi}+\frac{\sin 2\theta_1}{2\pi}\right] + P_2\left[\frac{\theta_2}{\pi}-\frac{\sin 2\theta_2}{2\pi}\right] \quad (5)$$

with

$$\theta_1 = \cos^{-1}\left(1-\frac{2x}{d_1\alpha}\right) \quad \theta_2 = \cos^{-1}\left[1-\frac{2(x-X_1)}{d_2\alpha}\right] \quad (6)$$

Let $x = X_2$ be the displacement of the LADAR at which target 1 just fails to occlude target 2. In this case, geometrical considerations give

$$X_2 = \frac{(s-q)(d_2-d_1)}{d_2} + d_1\alpha \quad (7)$$

4) **LADAR displacement** $2r_1 \leq x < X_2$ **(figure 7(c)).** The power received in the displacement interval $2r_1 \leq x < X_2$ results from the single footprint in figure 7(c):

$$P_{(2r_1\leq x<X_2)} = P_2\left(\frac{\theta_2}{\pi}-\frac{\sin 2\theta_2}{2\pi}\right)$$
$$\theta_2 = \cos^{-1}\left[1-\frac{2(x-X_1)}{d_2\alpha}\right] \quad (8)$$

5) **LADAR displacement** $x \geq X_2$ **(figure 7(d)).** Finally target 2 is fully illuminated and the LADAR has been displaced enough, so that no part of the footprint is occluded from the LADAR's receiver aperture. Then:

$$P_{(x\geq X_2)} = p_{(x\geq X_2)}\pi r_2^2 = P_2 = \text{constant} \quad (9)$$

$$r_1 \approx d_1\alpha/2 \quad r_2 \approx d_2\alpha/2 \quad (10)$$

where α is the beam width of the transmitted laser.

Equations 2, 4, 5, 8, and 9 between them, when θ_1 and θ_2 are replaced by their respective functions of x, describe the complete expected received amplitude profile as the LADAR's transmitted laser is scanned past a range discontinuity. In figure 8 (the red dotted profile), the amplitude profile is plotted versus the illuminated footprint displacement. Compared with the measured amplitude in figure 5, the estimated profile in figure 8 (the red dotted profile) is similar and the minimum value in the amplitude is almost the same, which proves the theoretical model to be correct. However the width of the change in the amplitude curve in the actual case (figure 5) is a little smaller than that in the simulated case (figure 8, the red dotted profile). The possible reason of the difference is due to the assumption that the laser energy is uniformly distributed over the beam cross section, which probably is not true in reality. In reality, the laser energy concentrates on around the center of the beam cross section, rather than normally distributed, which causes the real α, the beam width of the transmitted laser, is smaller than its labelled value and hence causes the difference in both figures.

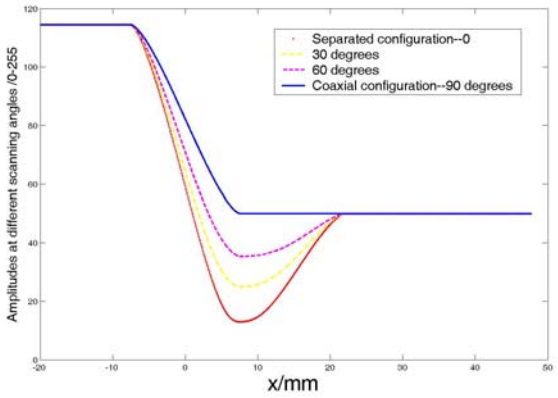

Fig. 8. Estimated amplitude profiles of separated transceiver configuration and "coaxial" configuration LADARs. In this case, the values of involving parameters are: $d1 = 5.8$m, $d2 = 12.6$m, $P1 = 115$, $P2 = 50$ and $s - q = 2.9$cm.

In Figure 8, individual estimated amplitude profiles corresponding to a certain scanning angle of the LADAR relative to the sensed target are shown for particular values of $d1$, $d2$, $P1$, $P2$, α and $s-q$. In this paper, the scanning angle θ is defined as the angle between the direction of the transmitted laser beam and the center line of the transceiver of the LADAR. When the LADAR scans, each θ corresponds a bearing angle (the angle the LADAR's mirror rotates about the vertical axis). The relationship between the scanning angle and transceiver configuration is explained in figure 9. In figure 9(c), the scanning angle 0^o corresponds to the separated transceiver configuration in figure 4(a) while in figure 9(a) the scanning angle is 90^o, corresponding to the "coaxial" type configuration in figure 4(b). Figure 9(b) shows the general case with scanning angle θ. As the scanning angle increases, the minimum value of the amplitude profiles increases which means potential elimination of the measurement error at a certain angle. If the scanning angle reaches 90^o, which corresponds to the case in figure 4(b), the transceiver configuration effectively becomes "coaxial" with respect to the vertical edge formed by the target/background and the minimum in the amplitude profile disappears (as shown in figure 8, the blue solid profile).

The above analysis is made to the 3D LADAR scanner in figure 1(b). For the 3D LADAR in figure 1(c), only one

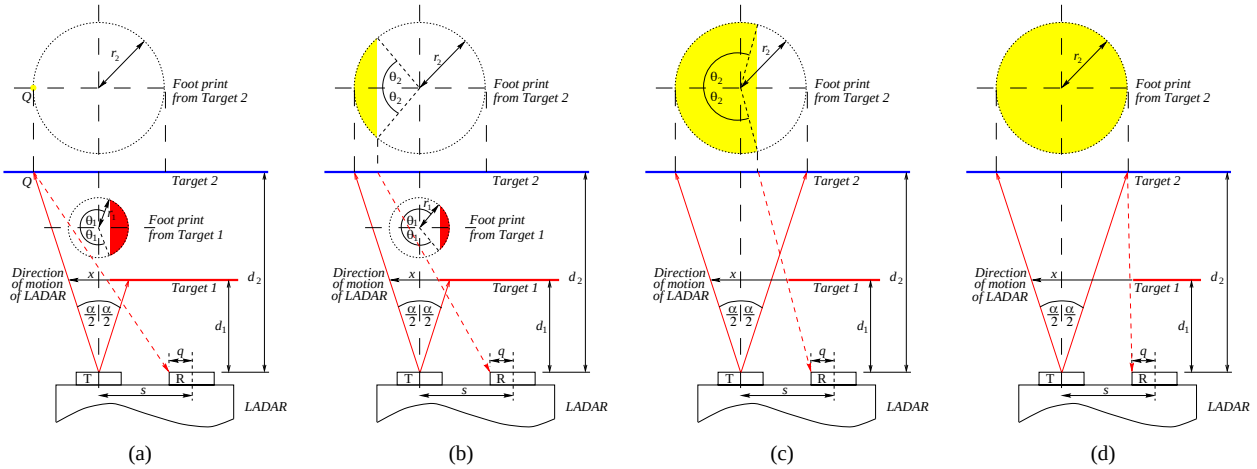

Fig. 7. (a) Point Q on target 2 just enters the field of view of the receiver aperture. (b) Light is now received from both targets 1 and 2.(c) Target 1 is no longer illuminated. Target 2 is partially occluded by target 1, due to transceiver separation s. (d) Light is now received from target 2 only, with no occlusion from target 1.

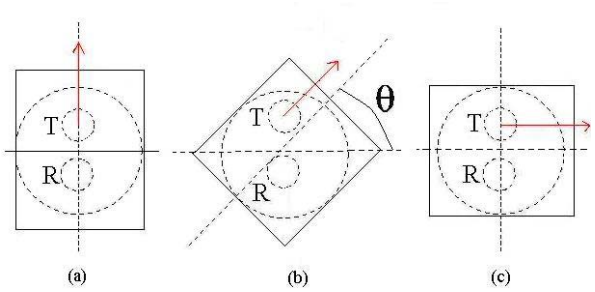

Fig. 9. Top view of LADAR scanning mirror. 'T,R' denote the LADAR's transmitter and receiver and the red arrows denotes the direction of transmitted laser. (a) $\theta = 90^o$, (c) $\theta = 0^o$ and (b) general case.

thing is different, which is that its rotating mirror rotates together with the transceiver and their relative position is constant. That means, for this kind of LADAR scanner, the transceiver is always "separated" (as the configuration in figure 9(c)) no matter what the LADAR's real bearing angle is. When this LADAR scans past a vertical edge as the one in figure 4, the estimated profile always has the form of the red dotted curve in figure 8.

V. Causes of Range Errors

To avoid range errors the minimum amplitude in the profile must be increased to a value above the minimum detectable amplitude value of the LADAR. In this section, the theoretical model will be analyzed to determine the effect of different LADAR design parameters and environmental parameters which can cause the received amplitude to fall below a predefined minimum value.

For the 3D LADAR scanner in figure 1(b), the fundamental parameter is the scanning angle θ of the LADAR. For the 3D LADAR in figure 1(c), it is not affected by this parameter at all since the transceiver is always "separated". In figure 8, by rotating the scanning mirror of the LADAR from 0^o to 90^o (figure 9), the minimum amplitude keeps increasing. In figure 10, the estimated signal amplitude is shown versus the sliding distance (x in mm) and the scanning angle (in degrees), which corresponds to different transceiver configuration in figure 9.

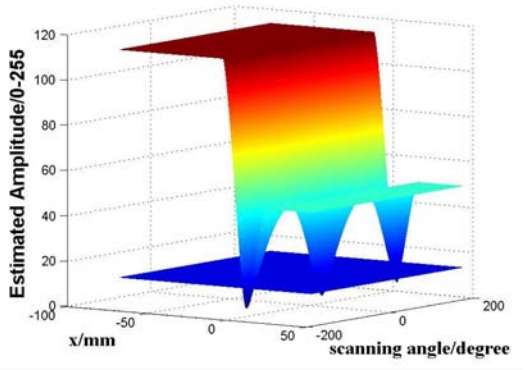

Fig. 10. Estimated signal amplitude versus the sliding distance x and the scanning angle θ. The other parameters used were $d1 = 5.8$m, $d2 = 12.6$m, $P1 = 115$, $P2 = 50$, $s - q = 2.9$cm and $\alpha = 3mrad$. The minimum detectable amplitude of the LADAR is plotted as the plane with $amplitude = 18$.

In figure 10, the minimum detectable amplitude of this Riegl LADAR is assumed to be 18[6], and as the scanning angle θ reaches $(n+1/2)\pi$ $rads$ (n integer), the minimum amplitude will be larger than 18 and then no range error will occur. In figure 11, the minimum amplitude in each amplitude profile corresponding to a scanning angle in figure 10 is plotted versus the bearing angle. Compared to the minimum detectable amplitude of the LADAR (the dotted line with amplitude=18), it can be seen that, the minimum will be larger than the minimum detectable amplitude and no range error will occur if $-160^o \leq \theta \leq -20^o$ and $20^o \leq \theta \leq 160^o$. Since the minimum detectable amplitude of each LADAR is different, the particular angular bearing range in which the range error will disappear depends on this value for the given device. For LADARs which

[6]Found by experiment.

maintain a constant separation between the transmitter and receiver (figure 1(c)), the range errors can always occur.

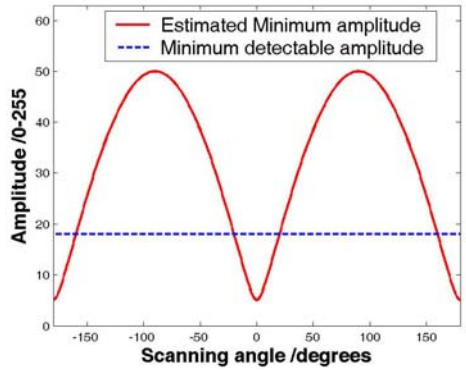

Fig. 11. Minimum amplitudes versus the scanning angle θ. The minimum detectable amplitude of the LADAR is plotted as the line with $amplitude = 18$.

The second parameter to be analyzed is a sensor parameter, $s - q$ (the transceiver separation) in equation 3. Both LADARs are affected by this parameter. As expected, figure 12 shows that by decreasing $s - q$, the minimum amplitude value can also be increased, thus decreasing the chances of false range values. During LADAR design, this

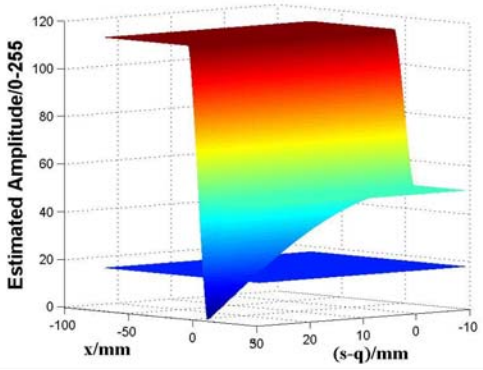

Fig. 12. Estimated signal amplitude versus the sliding distance x and the sensor parameter $s - q$. The minimum detectable amplitude of the LADAR is plotted as the plane with $amplitude = 18$.

parameter should be kept as small as possible while keeping the transmitter and receiver still separated to guarantee that all of the transmitted light leaves the LADAR.

Further parameters which affect the minimum value of the received amplitude are environmental, namely the distances and the reflectivity of the targets which form the scanned vertical edge. Again, both LADARs are affected by these parameters. If we decrease the distance of the background target so that the two targets are closer to each other, the minimum amplitude value is also increased. This makes sense since if the two targets are put at the same distance, the front target cannot occlude the reflected laser from the background target. In another case, when the received power P_2 from the background target is increased (corresponding to a higher reflectivity of that target), the minimum amplitude value is then also increased. It is interesting to note that for almost all combinations of edge separation $d_2 - d_1$, increasing the reflectivity of any one of the surfaces does not significantly increase the minimum in amplitude, as shown in figure 13.

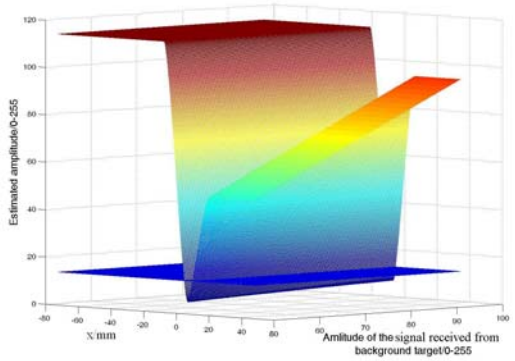

Fig. 13. Estimated signal amplitude versus the sliding distance x and the amplitude of signal received from the background target. The minimum detectable amplitude of the LADAR is plotted as the plane with $amplitude = 18$.

VI. Results

Finally, some experimental results are presented. Firstly, a semi-structured, outdoor environment (a car park area within the NTU campus) is used. Figure 14 shows a received amplitude image recorded from the 1D-sensor based LADAR in this environment. In figure 14, a black

Fig. 14. An intensity image of an semi-outdoor environment from the 1D-sensor based 3D LADAR. 'A' in the figure denotes a container.

container (position 'A') and the behind white wall form an edge where the occlusion effect could possibly occur in a LADAR scan. The ranges of the container and the wall were recorded and so were the received signal amplitudes. With this information, as shown in figure 15, an amplitude profile (the red amplitude profile denoted as "Estimated amplitude" in the legend) similar to those in figure 8 by using the theoretical model was produced. We can see that the minimum expected amplitude value in this case is lower than the LADAR's minimum detectable amplitude. Hence, in this case, range errors are expected at the edge. Compared with the actual amplitude data (the blue dotted profile) in the same figure, it can be seen that the shape and minimum of the amplitude in both actual and estimated profiles are almost same except that the width of the change in the estimated amplitude is larger than that in the actual one, for the probable reason that the actual laser beam width is larger than the theoretical one used in the estimation.

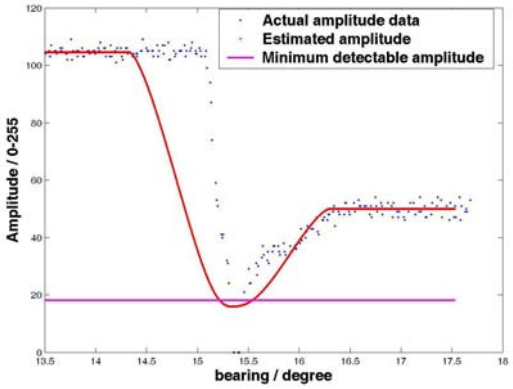

Fig. 15. Estimated amplitude profile from the middle row (elevation angle is 40^o) of the scan in figure 14 compared with the actual amplitude profile.

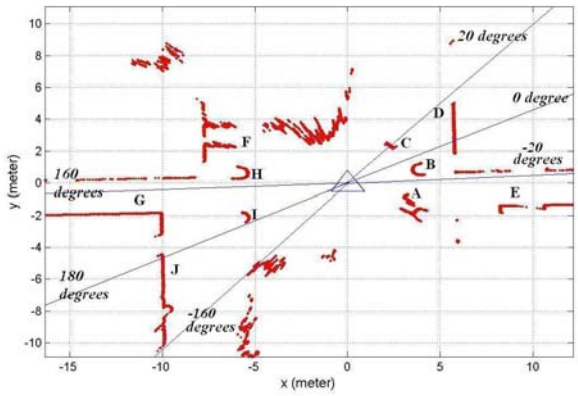

Fig. 16. Plan view of the range data from the middle row (elevation angle is 40^o) of figure 14. The small blue triangle denotes the position of the LADAR. The red lines are range data. Capital letters A to J denotes objects in the environment, in which A denotes crouching people, B, H, I are pillars, C is the container, D is a background wall, F denotes bicycles, E, G are a corridor and J is another wall. The blue lines marked $-20^o, 0^o$ etc are scanning angle bounds defining areas where the occlusion may occur (See figure 11).

Figure 16 shows the plan view of the range data from the middle row (elevation angle is 40^o) of figure 14. According to figure 11, false range values may occur at certain scanning angle ranges, which are $-180^o < \theta < -160^o$, $-20^o < \theta < 20^o$ and $160^o < \theta < 180^o$ etc and these reginos are marked on figure 16. The edge formed by the container and the wall falls in the scanning angle range $-20^o < \theta < 20^o$ and then false range values are expected. Figure 17 shows the signal amplitude and the range data from the same row versus the LADAR's bearing angle to depict the false range values at the edge . It can be seen that at the edge, a minimum in amplitude occurs and its value is below 18, the minimum detectable amplitude of the LADAR, producing false range estimates as expected. At this point, the range value should be replaced with its prediction if the range data is to be used in some feature detection methods[12].

Another experiment was carried out in an indoor environment. Figure 18 shows an intensity image recorded by the 3D LADAR in figure 1(c) in the same laboratory as in figure 2. For this LADAR, the scanning bearing angle is irrelative to the occlusion effect.

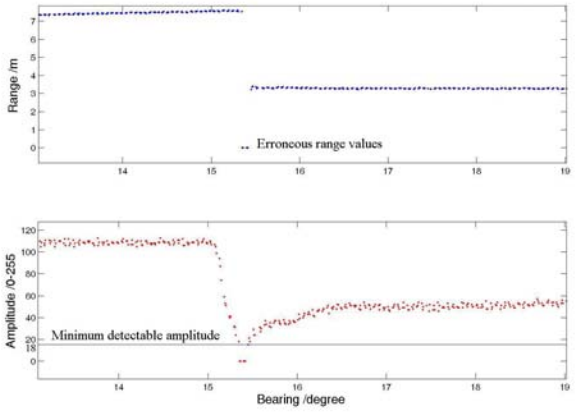

Fig. 17. The actual range data and the signal amplitude data versus bearing from the same row (elevation angle is 40^o) of figure 16.

Fig. 18. Received signal amplitude image recorded in the same laboratory environment in figure 2 by the 3D LADAR in figure 1(c). 'A' denotes a container.

In the environment, a black container (denoted 'A' in the intensity image) formed an edge with the behind white door. Again, the distances of the container and the door and the amplitudes of signals from the two targets were recorded by the LADAR. With this information, an amplitude profile which is similar to the red dotted one in figure 8 by using the theoretical model was produced, as shown in figure 19 (estimated amplitude profile 1). From this profile we can predict that the minimum amplitude value in this case is lower than the LADAR's minimum detectable amplitude and hence range error is predicted to appear.

In the actual data, amplitude drops below the LADAR's minimum detectable amplitude and range errors occur at the edge, which corresponds to the model.

From the analysis in section V, four parameters (the scanning angle θ, the transceiver separation $s - q$, the distances and the reflectivity of the targets which form the scanned vertical edge) can be tuned so that the minimum amplitude value at an edge can be increased and hence range errors can be avoided. For this 3D LADAR, the effect is irrelative to the bearing angle and it is impossible to change the parameter $s - q$. Hence, here we changed the environmental parameters–the reflectivity and distance of the target and investigated the effects on occlusion. First, the black container was covered by a white canvas so

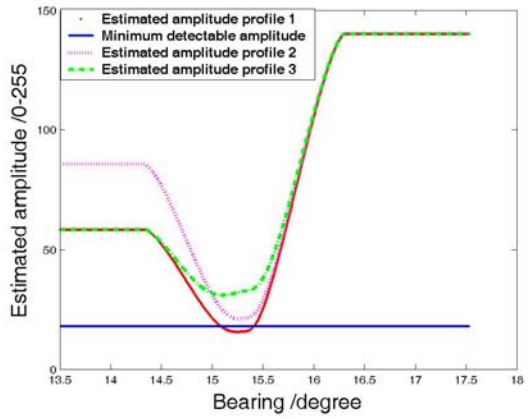

Fig. 19. *Estimated amplitude profiles: 1 corresponding to the middle row (elevation angle is 40^o) of figure 18; 2 corresponding to the case of changing the black container in figure 18 to white; 3 corresponding to the case of increasing the distance of the black containter in figure 18.*

that its reflectivity became higher. From the analysis about the effect of different reflectivity on amplitude profile, the minimum amplitude should increases a little as increasing the reflectivity of either surface. By changing the amplitude information only, we use the theoretical model to estimate the amplitude profile again and it is shown in figure 19 (Estimated amplitude 2). In the profile, although the amplitude from the front target is increased a lot, the minimum amplitude increases only by a small amount, but remains above the minimum detectable value of the sensor, and hence the range error should be avoided.

The white canvas cover was then removed from the black container and we reduced the distance between it and the white door behind it. By using this information, the amplitude profile was estimated again and shown in figure 19 (Estimated amplitude profile 3). In the profile, the minimum amplitude is increased and much larger than the minimum detectable value of the LADAR. Similar actual range and amplitude curves to that in figure 17 but with the amplitude at the edge above the minimum detectable value of the sensor and no range errors are omitted.

From the above analysis and results, it can be seen that the theoretical model is effective in predicting range errors caused by occlusion. After the range errors are detected, it is necessary to replace these erroneous points with predictions when the LADAR is used in feature detection applications [12], [8].

VII. Conclusion

This paper evaluates false range values caused by occlusion effects when using LADARs with non-coaxial transceiver configurations. It has been shown analytically and experimentally that a minimum in the received signal power will occur, which can be below the minimum operating signal power necessary for correct operation and hence cause erroneous range readings. For applications such as feature detection and data association, this effect will introduce unwanted measurement errors and can cause the failure of feature detection algorithms and range noise reduction techniques. However, by using the proposed received signal power model, such erroneous range values can be predicted and detected before further processing.

Also, from this model, it can be seen that the minimum received signal power depends on sensor parameters such as the transceiver aperture separation and the scanning angle, as well as environmental parameters such as the reflectivity and separation of the targets. This dependency information is important for LADAR users as well as LADAR designers and allows them to avoid or, at least predict false range data caused by occlusion. This paper has shown that the chances of occlusion errors can be minimized by minimizing the separation of the LADAR's transceiver at the design stage. Further, a large separation of the targets being sensed is much more likely to cause false estimation than the reflective qualities of the targets themselves. Hence the derived models can be used to guarantee that all range values at edges will be sensed correctly within certain target separation bounds.

Acknowledgment

This work was carried out under a collaboration between SIMTech and NTU, Singapore. We also acknowledge Professor Wang Han from NTU and his student Mr. Wang Xiao for their help.

References

[1] *M. D. Adams*, Sensor modelling, design and data processing for autonomous navigation. *World Scientific, 1999.*

[2] *J. A.Reina, "Characterization of a radial laser scanner for mobile robot navigation,"* Proc.IEEE/RSJ Int. Conf. on Intelligent robots and systems, *1997.*

[3] *Cang.Ye and Johann.Borenstein, "Characterization of a 2-d laser scanner for mobile robot obstacle negotiation,"* International Conference on Robotics and Automation, *May 2002.*

[4] *S. Clark and G. Dissanayake, "Simultaneous localisation and map building using millimetre wave radar to extract natural features,"* Proceedings of International Conf. on Robotics and Automation (ICRA'99), *pp. 1316–1321, May 1999.*

[5] *T. Einsele, "Localization in indoor environments using a panoramic laser range finder," Ph.D. dissertation, TU München, Fakultät für Elektro- und Informationstechnik, 2002.*

[6] *E. N. Jose Guivant and S. Baiker, "Autonomous navigation and map building using laser range sensors in outdoor applications,"* Journal of Robotic Systems, *no. 10, October 2000.*

[7] *Juan Nieto, Jose Guivant, and Eduardo Nebotand Sebastian Thrun, "Real time data association for fastslam,"* Proc. IEEE Int. Conf. Robotics and Automation, *2003.*

[8] *K.R.S. Kodagoda, W.s. Wijesoma, and A.P. Balasuriya, "Road curb and intersection detection using a 2d lms,"* Proceedings of the IEEE/RSJ International Conference on Intelligent Robots and Systems (IROS'02), *pp. 19–24, 2002.*

[9] *Martial.Hebert and Eric.Krotkov, "3-d measurements from imaging laser radars: How good are they?"* Image and Vision Computing, *no. 3, 1992.*

[10] *N. Pears and P. Probert, "Active Triangulation Rangefinder Design for Mobile Robotics," in* Int. Conf. Intelligent Robots and Systems, *1992.*

[11] *Raj Madhavan, Hugh Durrant-Whyte, and Gamini Dissanayake, "Natural landmark-based autonomous navigation using curvature scale space,"* Proceedings of International Conf. on Robotics and Automation (ICRA'02), *May 2002.*

[12] *Sen. Zhang, Lihua. Xie, Martin. Adams, and Fan. Tang, "Geometrical feature extraction using 2d range scanner,"* Proceedings of the Fourth International Conference on Control and Automation, *June 2003.*